ENGINEERING TRANSACTIONS • *Engng. Trans.* • **43**, 3, 397–411, 1995
Polish Academy of Sciences • Institute of Fundamental Technological Research

DESCRIPTION OF CREEP STRAIN ANISOTROPY OF THE LIGNOSTONE IN THE FORM OF TENSOR POLYNOMIAL AND A MODIFIED TENSOR POLYNOMIAL

M. CZECH (BIAŁYSTOK)

The results of creep investigations of the lignostone under axial compression are presented in the paper. The specimens were cut off from the lignostone bars at different angles to the main orthotropy axis. The tensor polynomial in the form (1.2) and the modified tensor polynomial in the form (1.3) were used to describe creep strain for different angles of cutting the specimens. The first and the third terms of the polynomials provide a correct description in both methods, however a better description has been obtained for the second one.

1. INTRODUCTION

Solution of initial-boundary value problems as well as technological problems require the knowledge of physical and mechanical properties of the materials used, both the short-term and the long-term ones [1].

The aim of the paper is the identification of creep processes of a nonlinear visco-elastic orthotropic body, that is the formulation of mathematical models, determination of model parameters and verification of the correct description for the models proposed.

The tensor polynomial in the form (1.1) describing the instantaneous strain of anisotropic body is used by many authors, for instance [2, 3]

$$\varepsilon_{ij} = a_{ijkl}\sigma_{kl} + a_{ijklmn}\sigma_{kl}\sigma_{mn} + a_{ijklmnop}\sigma_{kl}\sigma_{mn}\sigma_{op} + \dots \tag{1.1}$$

The mathematical model in the form (1.2) describing creep of an anisotropic body is applied in many papers [3] by analogy to Eq. (1.1)

$$\varepsilon'_{ij}(t) = \sigma'_{kl}\left[a'_{ijkl} + \int_0^t K'_{ijkl}(t-\tau)\,d\tau\right] + \sigma'_{kl}\sigma'_{mn}\left[a'_{ijklmn} + \int_0^t K'_{ijklmn}(t-\tau)\,d\tau\right] \tag{1.2}$$

$$(1.2)\ [\text{cont.}] \qquad + \sigma'_{kl}\sigma'_{mn}\sigma'_{op}\left[a'_{ijklmnop} + \int_0^t K'_{ijklmnop}(t-\tau)\,d\tau\right] + \ldots, \qquad i,j,k,l,m,n,\ldots = 1,2,3,$$

where a'_{ijkl}, a'_{ijklmn}, ... – components of linear and nonlinear anisotropy tensors (constant deformability tensors) for transformed system, K'_{ijkl}, K'_{ijklmn}, ... – components of linear and nonlinear creep kernel tensors, σ'_{kl}, σ'_{mn}, ... – components of the transformed system stress tensor. Creep can be described by taking a sufficient number of terms (1.2). The number of constants required to determine Eqs. (1.2) rapidly rises with the number of terms, what increases the number of experimental tests. For those reasons two terms only are taken. However, such limitation not always gives the correct description.

The modified tensor polynomial in form (1.3) as the second mathematical model is applied in the paper

$$(1.3) \qquad \varepsilon'_{ij} = a'_{ijkl}\sigma'_{kl} + a'_{ijklmn}\sigma'_{kl}\sigma'_{mn} + \ldots + (\sigma'_{kl})^{\alpha_1}\int_0^t K'_{ijkl}(t-\tau)\,d\tau$$

$$+(\sigma'_{kl}\sigma'_{mn})^{\alpha_2}\int_0^t K'_{ijklmn}(t-\tau)\,d\tau + \ldots, \qquad i,j,k,l,m,n,\ldots = 1,2,3,$$

where $\alpha_n = [1 + (n-1)r]/n$, n-th term of polynomial, $r = 3$. The other notations are the same as in the formula (1.2).

2. Experimental tests

The cuboidal specimens for creep tests under compression are presented in Fig. 1. Loading directions are coincident with directions at what the samples were cutt off from the lignostone bar, and they are also presented in the Fig. 1.

The manufacturing conditions are given in [4]. Specimens for creep tests were made of birch-wood lignostone with the density 990 kg/m^3 and compression ratio 1.45.

The tests were performed for five different values of α. Five specimens for each stress level were made for $\alpha = 0°$ and $\alpha = 90°$ (five stress levels), and three specimens for each stress level were made for $\alpha = 30°$, 45° and 60° (four stress levels). Prior to testing, the specimens were seasoned in the air of humidity (65 ± 2.5)% and at the temperature of (293 ± 3) K. Creep tests under compression were performed under identical conditions.

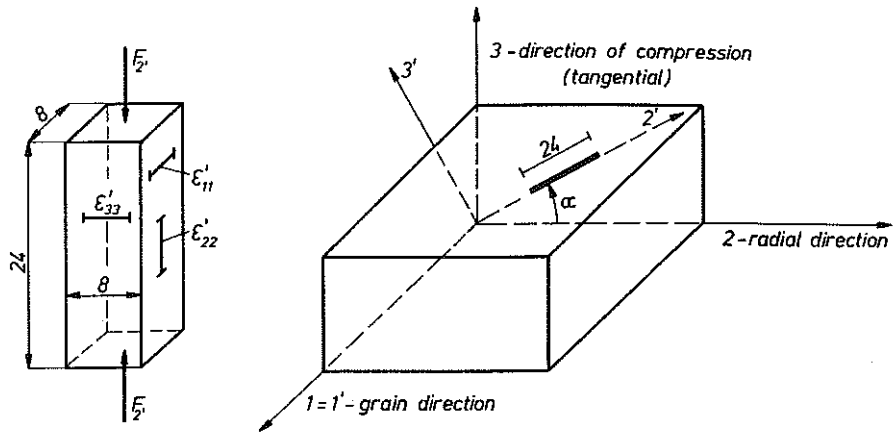

FIG. 1. Test specimens and directions at which they were cut off from the lignostone bar; a) load direction and strain measurement directions, b) material orthotropy axis and off-cut directions of the specimens.

The creep strains were measured by strain gauges with accuracy of 1 μm for small values of strains; larger strains were measured by means of dial gauges with accuracy of 10 μm and 100 μm.

3. TEST RESULTS

The results of creep tests under compression in the plane 2-3 are presented for instance in the Figs. 2–4 for longitudinal strains, and for transverse strains they are presented in the Figs. 5–10.

4. DESCRIPTION OF CREEP IN THE FORM OF TENSOR POLYNOMIAL

The global strain ε'_{ij} will be a sum of the instantaneous strain and the creep strain

$$\varepsilon'_{ij}(t, \sigma_{22}) = \varepsilon'_{ij}(0, \sigma'_{22}) + \varepsilon'^{c}_{ij}(t, \sigma'_{22}). \tag{4.1}$$

Formula (4.2) describes the instantaneous strain resulting from Eqs. (1.1) or (1.2)

$$\varepsilon'_{ij}(0, \sigma'_{22}) = a'_{ij22}\sigma'_{22} + a'_{ij222222}\sigma'^{3}_{22} = A'_{ij22}\sigma'_{22}/R + A'_{ij222222}(\sigma'_{22}/R)^3, \tag{4.2}$$

where $R = R_{22} = 44.7$ MPa – compression strength in the direction of axis 2.

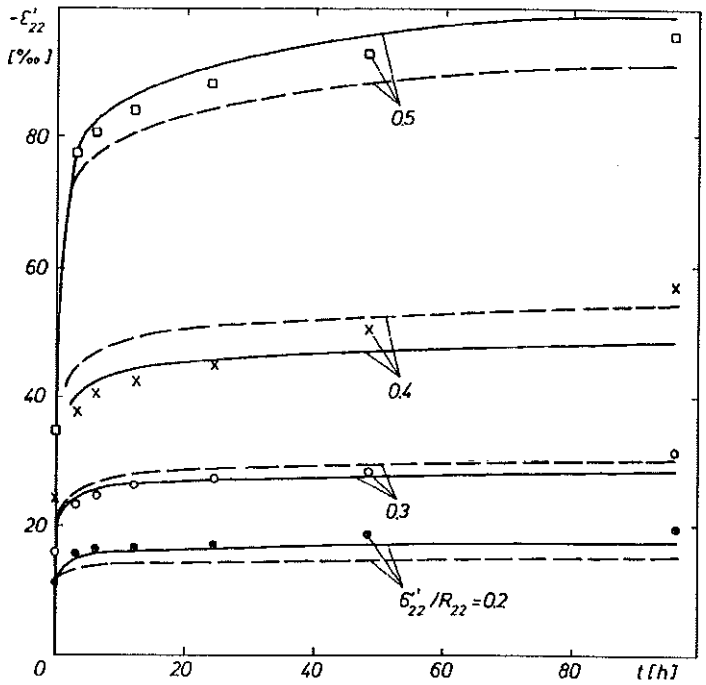

FIG. 2. Creep ε'_{22} curves of lignostone for $\alpha = 30°$; points – experimental data, dashed lines – theoretical curves acc. to (1.2), full lines – theoretical curves acc. (1.3).

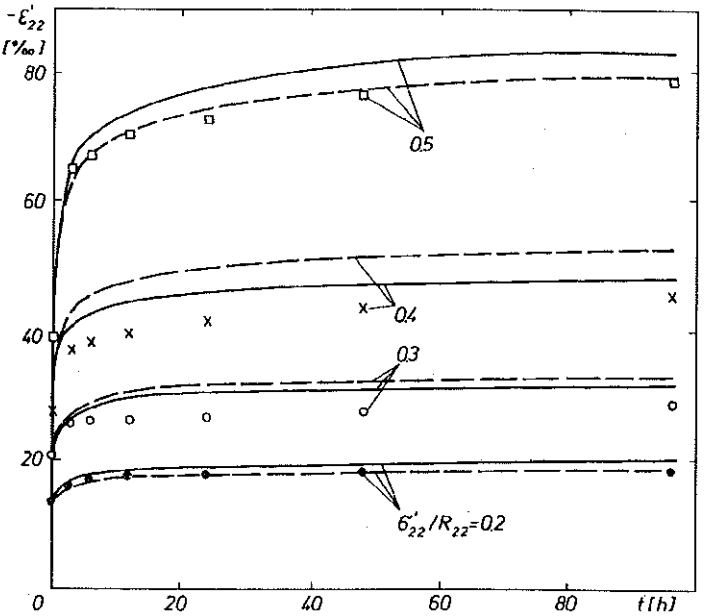

FIG. 3. Creep ε'_{22} curves of lignostone for $\alpha = 45°$; points – experimental data, dashed lines – theoretical curves acc. to (1.2), full lines – theoretical curves acc. (1.3).

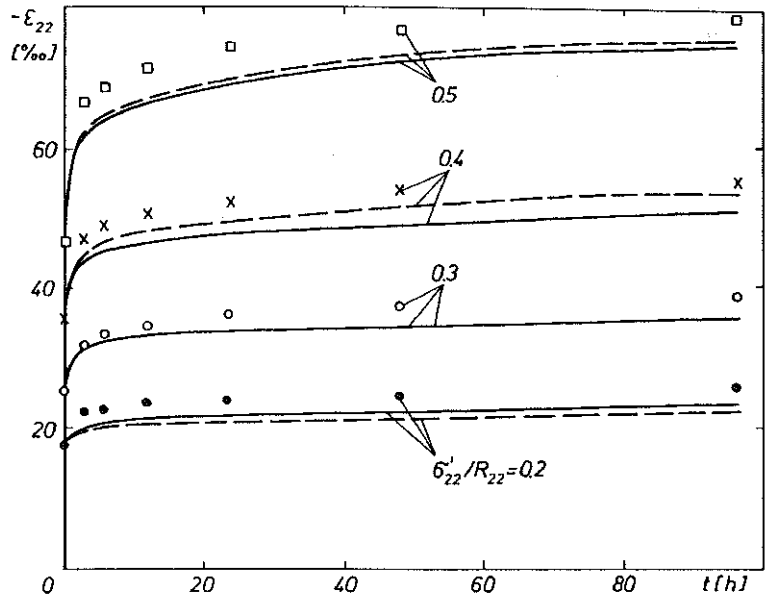

FIG. 4. Creep ε'_{22} curves of lignostone for $\alpha = 60°$; points – experimental data, dashed lines – theoretical curves acc. to (1.2), full lines – theoretical curves acc. (1.3).

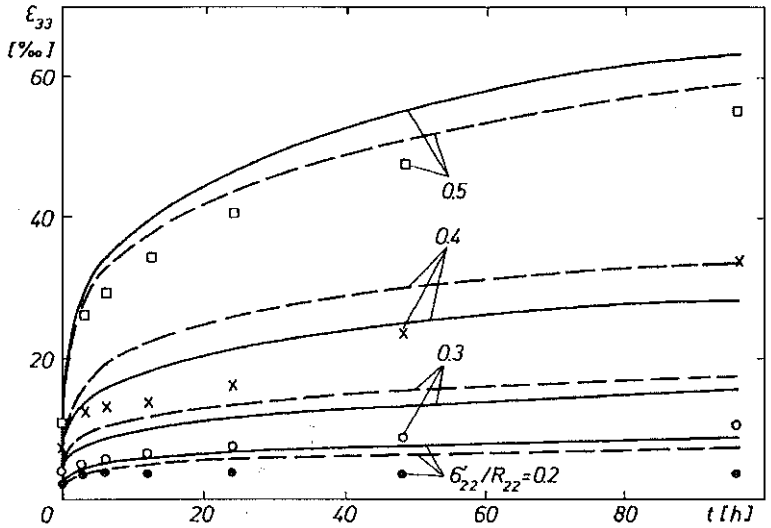

FIG. 5. Creep ε'_{33} curves of lignostone for $\alpha = 30°$; points – experimental data, dashed lines – theoretical curves acc. to (1.2), full lines – theoretical curves acc. (1.3).

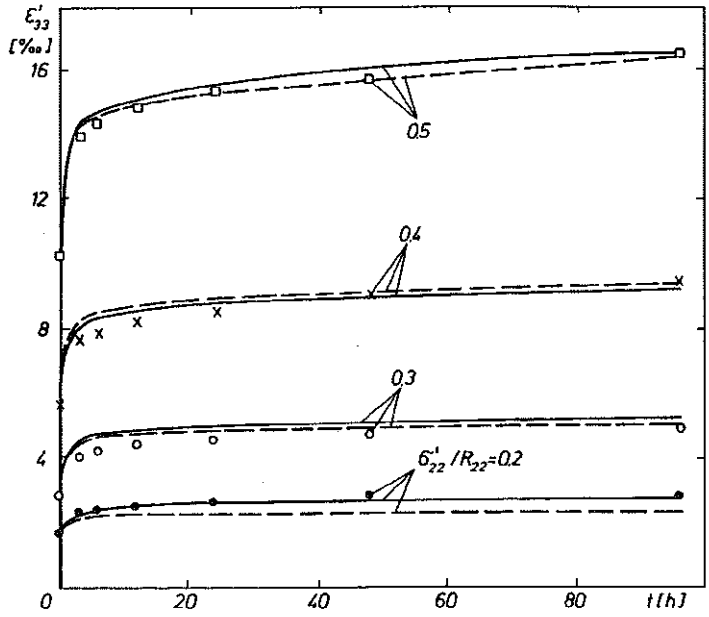

FIG. 6. Creep ε'_{33} curves of lignostone for $\alpha = 45°$; points – experimental data, dashed lines – theoretical curves acc. to (1.2), full lines – theoretical curves acc. (1.3).

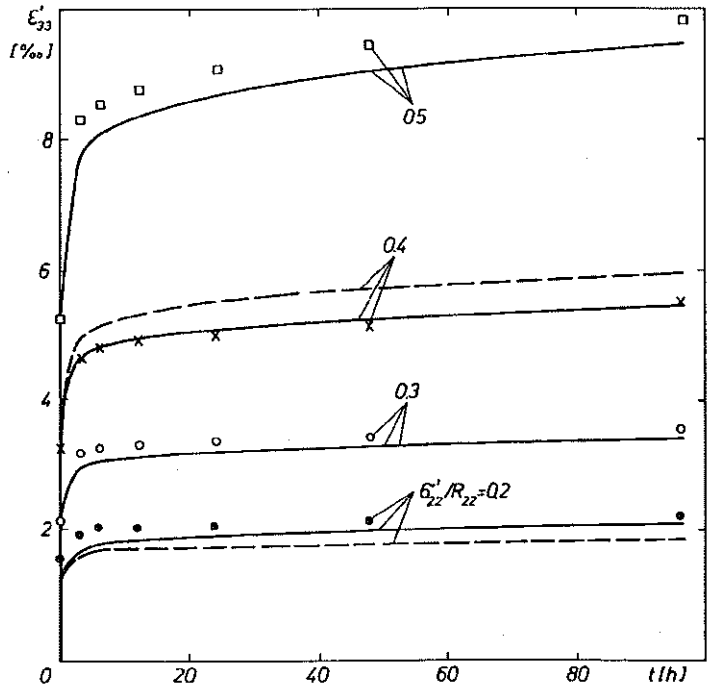

FIG. 7. Creep ε'_{33} curves of lignostone for $\alpha = 60°$; points – experimental data, dashed lines – theoretical curves acc. to (1.2), full lines – theoretical curves acc. (1.3).

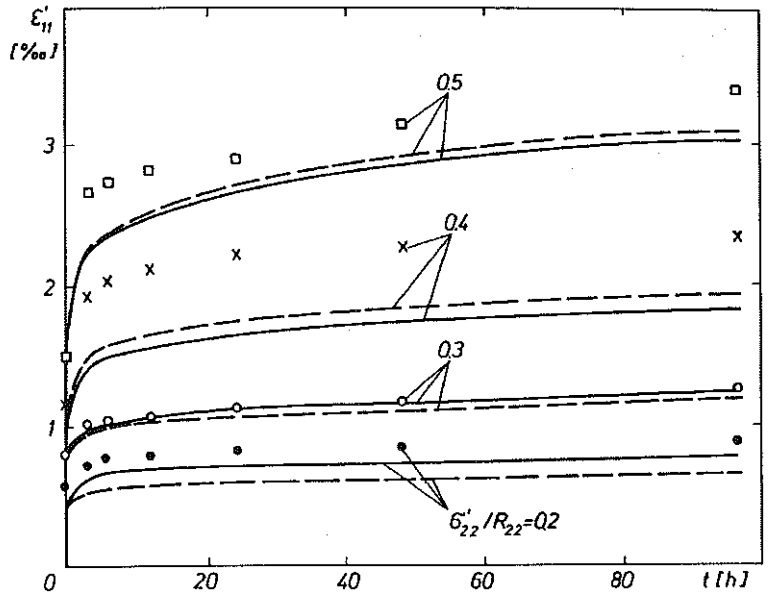

FIG. 8. Creep ε'_{11} curves of lignostone for $\alpha = 30°$; points – experimental data, dashed lines – theoretical curves acc. to (1.2), full lines – theoretical curves acc. (1.3).

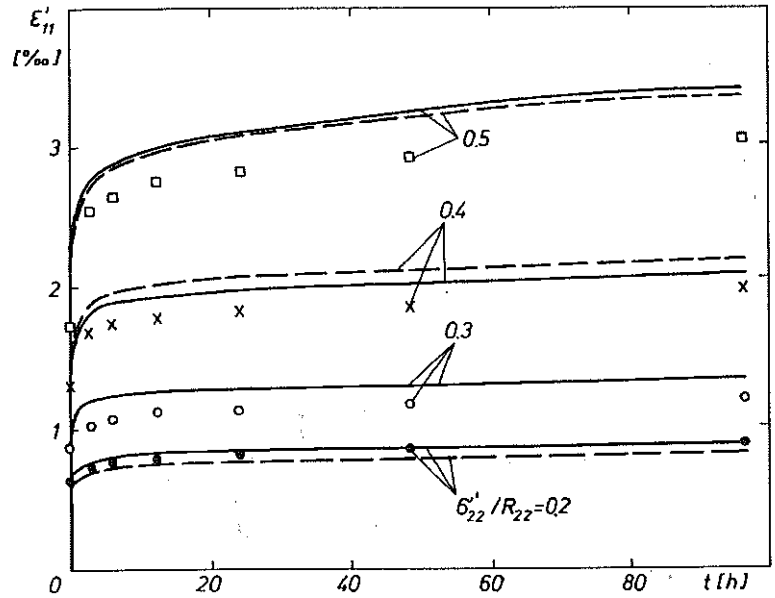

FIG. 9. Creep ε'_{11} curves of lignostone for $\alpha = 45°$; points – experimental data, dashed lines – theoretical curves acc. to (1.2), full lines – theoretical curves acc. (1.3).

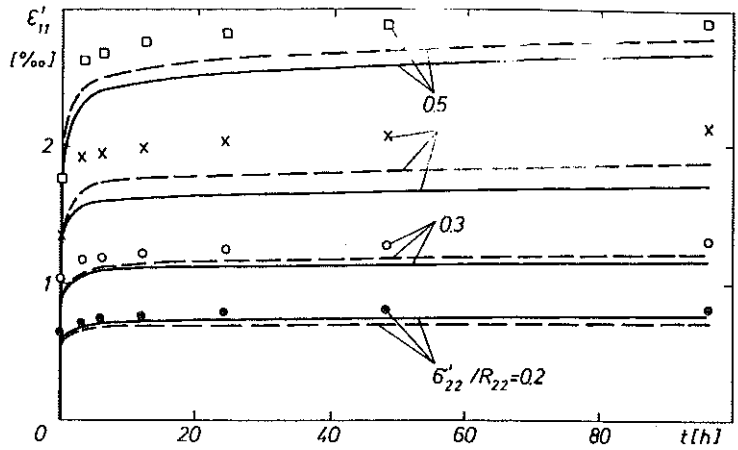

FIG. 10. Creep ε'_{11} curves of lignostone for $\alpha = 60°$; dots represent experimental data, broken lines – theoretical curves acc. (1.2), full lines – theoretical curves acc. to (1.3).

On the assumption of similarity of the creep curves, the creep strain is presented in the form:

$$\varepsilon'^{c}_{ij}(t, \sigma'_{22}) = f'_{ij}(\sigma'_{22}) g'(t). \tag{4.3}$$

Constant ratios $\varepsilon'^{c}_{ij}(\sigma'_{22})/\varepsilon'^{c}_{ij}(\sigma'_{22} = \sigma'^{\max}_{22})$ for different times have statistically proved the above assumption.

The function $f'_{ij}(\sigma'_{22})$ is assumed to have the form

$$f'_{ij}(\sigma'_{22}) = E'_{ij22}(\sigma'_{22}/R) + E'_{ij222222}(\sigma'_{22}/R)^3, \tag{4.4}$$

and the function

$$g'(t) = \int_0^t K'(t-\tau)\, d\tau, \tag{4.5}$$

where

$$\begin{aligned} K'(t-\tau) &= t_0^{-D} \overline{B} (t-\tau)^{D'-1} e^{-C'((t-\tau)/t_0)^{D'}}, \\ \overline{B}' &= B'C'D', \qquad t_0 = 1\,\mathrm{h}. \end{aligned} \tag{4.6}$$

Substituting (4.6) into (4.5) and integrating we obtain

$$g'(t) = B' \left[1 - e^{-C(t/t_0)^{D'}}\right]. \tag{4.7}$$

The function (4.7) is the so-called Kohlrausch function, and it can be also obtained from the modified standard model [4, 5].

The constants used in the formulae (4.2), (4.4) and (4.7) are determined by the least square method (LSM).

The constants appearing in the formulae (4.2) and (4.4) are transformed as follows:

$$
\begin{aligned}
a'_{ijkl} &= \alpha_{im}\alpha_{jn}\alpha_{ko}\alpha_{lp}a_{mnop}\,, \\
a'_{ijklnmop} &= \alpha_{ir}\alpha_{js}\alpha_{kt}\alpha_{lu}\alpha_{mv}\alpha_{nw}\alpha_{ox}\alpha_{py}a_{rstuvwxy}\,,
\end{aligned} \tag{4.8}
$$

where $i, j, \ldots, y = 1, 2, 3$.

Coefficients α_{ij} which are cosines of angles between the axes of the new coordinate system and the previous ones are equal (from Fig. 1) to

$$
\begin{aligned}
&\alpha_{11} = 1, && \alpha_{22} = \alpha_{33} = \cos\alpha, \\
&\alpha_{23} = \sin\alpha, && \alpha_{32} = -\sin\alpha, \\
&\alpha_{12} = \alpha_{13} = \alpha_{21} = \alpha_{31} = 0.
\end{aligned} \tag{4.9}
$$

The constants in the formula (4.7) are calculated for five angles. For other angles these constants can be calculated using a square interpolation (interpolation polynomial of Lagrange).

4.1. Description of ε'_{22} creep strain in longitudinal direction (load direction $i = j = 2$)

The values $i = j = 2$ are substituted into the formulae (4.1) to (4.4). The constants in the formulae (4.2), (4.4) and (4.7) are determined according to the LMS method.

Assuming the lignostone to be an orthotropic material and using the equations (4.8) and (4.9), some of the coefficients of Eq. (4.2) are found to have the form:

$$
\begin{aligned}
A'_{2222} &= a\cos^4\alpha + b\cos^2\alpha\sin^2\alpha + c\sin^4\alpha\,, \\
A'_{22222222} &= A\cos^8\alpha + B\cos^6\alpha\sin^2\alpha + C\cos^4\alpha\sin^4\alpha \\
&\quad + D\sin^6\alpha\cos^2\alpha + E\sin^8\alpha\,,
\end{aligned} \tag{4.10}
$$

where

$$
\begin{aligned}
&a = A_{2222}\,, && b = 2A_{2233} + 4A_{2323}\,, && c = A_{3333}\,, \\
&A = A_{22222222}\,, && B = 4A_{22222233} + 24A_{22222323}\,, \\
&C = 6A_{22223333} + 48A_{23232233} + 16A_{23232323}\,, \\
&D = 4A_{33333322} + 24A_{33332323}\,, && E = A_{33333333}\,.
\end{aligned} \tag{4.11}
$$

The coefficients appearing in the formula (4.4) will have a similar form. Constants $a, b, c, A, \ldots, E$ are determined by the LSM method.

The constants appearing in the formula (4.2) depend on the angle α according to formula (4.10), similarly to the constants in the formula (4.4). Their values for angles are given in the Table 1. The description of creep by the formulae (4.1) to (4.4) and (4.7) with the constants taken from Table 1 is illustrated in the Figs. 2 to 4 by the dashed lines.

4.2. Description of ε'_{33} creep in transverse direction ($i = j = 3$)

The values $i = j = 3$ are substituted into the formulae (4.1) to (4.4). The constants in the formulae (4.2), (4.4) and (4.7) are determined by the LSM method.

Assuming the lignostone to be an orthotropic body and using the equations (4.8) and (4.9), some of the coefficients of formula (4.2) are found.

$$
\begin{aligned}
&A'_{3322} = a + b\sin^2 2\alpha\,,\\
&A'_{33222222} = A\cos^8\alpha + B\cos^6\alpha\sin^2\alpha + C\cos^4\alpha\sin^4\alpha\\
&\qquad\qquad + D\cos^2\alpha\sin^6\alpha + E\sin^8\alpha\,,
\end{aligned}
\tag{4.12}
$$

where

$$
\begin{aligned}
&a = A_{2233}\,, \qquad b = \frac{1}{4}(A_{2222} - 4A_{2323} - 2A_{2233} + A_{3333}),\\
&A = A_{33222222}\,,\\
&B = 3A_{22223333} + A_{22222222} - 12A_{22222323} + 12A_{22332323}\,,\\
&C = 3A_{22222233} - 24A_{22332323} + 3A_{33333322} + 12A_{33332323}\\
&\qquad\qquad + 12A_{22222323} - 16A_{23232323}\,,\\
&D = 3A_{22223333} - 12A_{33332323} + 12A_{23332323} + A_{33333333}\,,\\
&E = A_{22333333}\,.
\end{aligned}
\tag{4.13}
$$

The coefficients appearing in the formula (4.4) will have a similar form.

The constants $a, b, A, \ldots, E$ are determined by the LSM method. The constants in formulae (4.2) and (4.4) were determined using Eqs. (4.12).

Their values are given in Table 1. The process of creep according to the formulae (4.1) to (4.4) and (4.7) with the constants taken from Table 1 is presented in the Figs. 5 to 7 (dashed lines).

Table 1. Constants in the Eqs. (4.2), (4.4) and (4.7).

ε_{ij}	Factors	α [°]				
		0	30	45	60	90
ε'_{22}	$A'_{2222} \cdot 10^3$	17.942	45.184	66.273	81.208	89.991
	$A'_{22222222} \cdot 10^3$	14.122	91.131	53.490	44.147	10.194
	$E'_{2222} \cdot 10^3$	0.075	0.163	0.352	0.643	1.035
	$E'_{22222222} \cdot 10^3$	3.832	6.770	6.515	4.246	0.137
	B'	31.722	76.19	42.73	94.03	52.391
	C'	0.242	0.645	0.591	0.186	0.697
	D'	0.370	0.209	0.336	0.193	0.262
ε'_{33}	$-A'_{3322} \cdot 10^3$	3.334	5.484	6.200	5.484	3.334
	$-A'_{33222222} \cdot 10^3$	1.220	55.543	63.040	18.037	4.702
	$-E'_{3322} \cdot 10^3$	0.665	0.393	0.302	0.393	0.665
	$-E'_{33222222} \cdot 10^3$	1.855	7.473	5.700	6.119	0.706
	B'	3.741	121.83	15.99	9.220	8.991
	C'	0.113	0.102	0.216	0.312	0.179
	D'	0.311	0.322	0.181	0.181	0.203
ε'_{11}	$-A'_{1122} \cdot 10^3$	1.135	2.121	3.107	2.756	2.405
	$-A'_{11222222} \cdot 10^3$	1.043	1.947	2.100	1.523	0.238
	$-E'_{1122} \cdot 10^3$	0.384	0.260	0.136	0.281	0.426
	$-E'_{11222222} \cdot 10^3$	3.968	6.332	8.158	7.106	0.838
	B'	1.314	4.009	2.250	3.362	6.340
	C'	0.189	0.238	0.269	0.269	0.184
	D'	0.279	0.217	0.214	0.105	0.151

4.3. Description of ε'_{11} creep in transverse direction ($i = j = 1$)

Values $i = j = 1$ are substituted into the formulae (4.1) to (4.4). The constants in the formulae (4.2), (4.4) and (4.7) are determined applying the LSM method.

Using the formula (4.8) for the lignostone treated as an orthotropic body, some coefficients of the formula (4.2) are found in the form

$$A'_{1122} = a + b\sin^2\alpha\,,$$

$$A'_{11222222} = A\cos^6\alpha + B\cos^4\alpha\sin^2\alpha + C\cos^2\alpha\sin^4\alpha + D\sin^6\alpha\,, \tag{4.14}$$

where

$$a = A_{1122}\,, \qquad b = A_{1133} - A_{1122}\,,$$

$$A = A_{11222222}\,, \qquad B = 3A_{11222233} + 12A_{11222323}\,, \tag{4.15}$$

$$C = 3A_{11223333} + 12A_{11332323}\,, \qquad D = A_{11333333}\,.$$

The coefficients appearing in the formula (4.4) will have a similar form. Constants $a, b, A, \ldots, D$ are determined by the LSM method. The constants appearing in (4.2), (4.4) are expressed as functions of angle α by means of Eqs. (4.14), and some of them are listed in Table 1. The process of creep given by Eqs. (4.1) to (4.4) and (4.7), with constants taken from Table 1, is illustrated by Figs. 8, 9 10 (dashed lines).

5. Description of creep by means of the modified tensor polynomial

The global strain $\varepsilon' m_{ij}$ is the sum of the instantaneous strain and the creep strain,

$$\varepsilon'^{m}_{ij}(t, \sigma'_{22}) = \varepsilon'^{m}_{ij}(0, \sigma'_{22}) + \varepsilon'^{cm}_{ij}(t, \sigma'_{22}). \tag{5.1}$$

Formula (4.2) yields the instantaneous strain $\varepsilon'_{ij}(0, \sigma'_{22})$ resulting from Eq. (1.3). The creep strain is presented in the form similar to (4.3),

$$\varepsilon'^{cm}_{ij}(t, \sigma'_{22}) = f'^{m}_{ij}(\sigma'_{22}) g'(t). \tag{5.2}$$

Function $f'^{m}_{ij}(\sigma'_{22})$ is assumed as follows:

$$f'^{m}_{ij}(\sigma'_{22}) = E'^{m}_{ij22}(\sigma'_{22}/R) + E'^{m}_{ij222222}\left((\sigma'_{22}/R)^3\right)^{7/3}, \tag{5.3}$$

and function $g'(t)$ is given by Eq. (4.7).

The constants appearing in formulae (4.2), (5.3) and (4.7) are determined by the LSM method. Constants appearing in formulae (4.2) and (5.3) depend on the angle α according to the Eqs. (4.8) and (4.9).

5.1. *Description of ε'^{m}_{22} creep in longitudinal direction (load direction $i = j = 2$)*

Formulae (5.1)–(5.3), (4.2) and (4.7) are used with $i = j = 2$. The constants appearing in Eqs. (4.2), (5.3) and (4.7) are found by means of the LSM method. Equations (4.9), (4.10) are now used to express the constants appearing in the formulae (4.2) and (5.3) as functions of angle α, similarly to the procedure used in Sec. 4.1. They were evaluated for several angles α and are given in Table 2. The process of creep as described by Eqs. (5.1)–(5.3), (4.2) and (4.7), with constants taken from Tables 1, 2, are drawn (in solid lines) in Figs. 2–4.

Table 2. Constants in Eq. (5.3).

ε_{ij}	Factors	α [°]				
		0	30	45	60	90
ε'_{22}	$E'^m_{2222} \cdot 10^3$	0.422	0.614	0.792	0.953	1.100
	$E'^m_{22222222} \cdot 10^3$	25.181	95.093	87.566	46.922	0.800
ε'_{33}	$-E'^m_{3322} \cdot 10^3$	0.901	0.861	0.848	0.861	0.901
	$-E'^m_{33222222} \cdot 10^3$	9.558	101.657	59.900	65.767	3.698
ε'_{11}	$-E'^m_{1122} \cdot 10^3$	0.955	0.878	0.800	0.800	0.800
	$-E'^m_{11222222} \cdot 10^3$	3.540	5.698	7.007	6.113	1.666

5.2. *Description of ε'^m_{33} creep in transverse direction* ($i = j = 3$)

Formulae (5.1)–(5.3), (4.2), (4.7) are used with the substitution $i = j = 3$. Constants appearing in (4.2), (5.3) and (4.7) are determined by the LSM method. Formulae (4.12), (4.13) are used to express the constants appearing in (4.2), (5.3) as functions of the angle α (similarly to Sec. 4.2); the constants are given (at several values of α) in Table 2. The creep curves described by formulae (5.1)–(5.3), (4.2) and (4.7) with constants taken from Tables 1, 2 are shown in Figs. 5–7 (solid lines).

5.3. *Description of ε'^m_{11} creep in transverse direction* ($i = j = 1$)

The values $i = j = 1$ are substituted in Eqs. (5.1)–(5.3), (4.2) and (4.7). The constants appearing in Eqs (4.2), (5.3), (4.7) are determined by the LSM method. Constants in Eqs. (4.2), (5.3) depend on the angles according to (4.14), (4.15) (similarly to Sec. 4.3), and their values determined for several angles α are given in Table 2. The creep curves following from Eqs. (5.1)–(5.3), (4.2), (4.7), with constants taken from Tables 1, 2 are presented in Figs. 8, 9, 10 (in solid lines).

6. Statistical verification of the mathematical models

To verify the accuracy of the description, let us calculate the mean ab-

solute and relative square errors are from the formulae

$$
\begin{aligned}
r_1 &= \left\{ \left[\sum_{i=1}^{n} \sum_{j=1}^{m} \left(\overline{y}_{ij}^{e} - y_{ij}^{t} \right)^2 \right] / nm \right\}^{1/2}, \\
r_2^r &= \left\{ \left[\sum_{i=1}^{n} \sum_{j=1}^{m} \left(\left(\overline{y}_{ij}^{e} - y_{ij}^{t} \right) / \overline{y}_{ij}^{e} \right)^2 \right] / nm \right\}^{1/2},
\end{aligned} \tag{6.1}
$$

where n – number of stress levels, m – number of instants at which the strain readings were made, $\overline{y}_{ij}^{e}$ – mean experimental strain at the i-th stress level and j-th strain reading, y_{ij}^{t} – theoretical strain.

The errors evaluated of by the formula (6.1) were compared with the absolute and relative deviations calculated by the formulae:

$$
\begin{aligned}
\Delta_1 &= t_{\alpha,\nu} \left\{ \left[\sum_{i=1}^{n} \sum_{j=1}^{m} \sum_{k=1}^{p} \left(y_{ijk}^{e} - \overline{y}_{ij}^{e} \right)^2 \right] / \nu \right\}^{1/2}, \\
\Delta_1^r &= t_{\alpha,\nu} \left\{ \frac{1}{\nu} \left[\sum_{i=1}^{n} \sum_{j=1}^{m} \sum_{k=1}^{p} \left(\left(y_{ijk}^{e} - \overline{y}_{ij}^{e} \right) / \overline{y}_{ij}^{e} \right)^2 \right] \right\}^{1/2},
\end{aligned} \tag{6.2}
$$

where $t_{\alpha,\nu}$ – the critical value of t-Student's distribution for α – significance level and $\nu = nmp - nm$ – degree of freedom, y_{ijk}^{e} – experimental strains for k-th repetition on i-th level of stress at j-th reading of strain.

Before these deviations vere calculated, the Cochran test was used to check the variance homogeneity. The results are compiled in Table 3.

7. Conclusions

1. The creep strains are nonlinear and the creep curves are similar. The accuracy of the applied mathematical models in the form of a tensor polynomial (TP) and a modified tensor polynomial (MTP) can be seen in Figs. 2 – 10 and Table 3.

2. Analysis of the results given in Table 3 leads to a conclusion that application of the MTP improves the accuracy of the approach.

3. The plot of the isochronous curves on the basis of Figs. 2 – 10 allows to conclude that, in the range of stresses $\sigma'_{22} < 0.3R_{22}$, the instantaneous strains and the creep strains are linear, hence they can be described by the linear theory of viscoelasticity in that range of stresses.

Table 3. Values for verification of the mathematical model.

ε_{ij}	Mathematical model	Statistical values	α [°] 0	30	45	60	90
ε'_{22}	T.P.	r_1 [‰]	0.955	4.247	3.396	2.527	2.491
		r_2^r	0.073	0.133	0.095	0.066	0.037
	M.T.P.	r_1 [‰]	0.395	2.643	2.625	2.895	3.000
		r_2^r	0.026	0.076	0.072	0.065	0.033
	Δ_1 [‰]		2.367	8.119	4.380	5.706	7.986
	Δ_2^r		0.180	0.250	0.131	0.148	0.113
ε'_{33}	T.P.	r_1 [‰]	0.128	3.636	0.433	0.304	0.397
		r_2^r	0.085	0.458	0.197	0.097	0.105
	M.T.P.	r_1 [‰]	0.131	3.409	0.402	0.266	0.416
		r_2^r	0.091	0.455	0.077	0.071	0.133
	Δ_1 [‰]		0.385	4.011	0.776	0.568	0.575
	Δ_2^r		0.278	0.499	0.213	0.158	0.174
ε'_{11}	T.P.	r_1 [‰]	0.114	0.285	0.143	0.151	0.175
		r_2^r	0.234	0.176	0.099	0.094	0.109
	M.T.P.	r_1 [‰]	0.118	0.311	0.138	0.217	0.224
		r_2^r	0.274	0.161	0.089	0.112	0.172
	Δ_1 [‰]		0.209	0.354	0.378	0.362	0.355
	Δ_2^r		0.448	0.256	0.300	0.250	0.192

REFERENCES

1. F. KOLLMAN, *Rheologie and Strukturfestigkeit von Holz als Rols und Werkstoff*, 3, 1961.
2. I.I. GOLDENBLAT, *Some problems in mechanics of deformable materials* [in Russian], Moscow 1955.
3. A.K. MALMEJSTER, W.P. TAMUZH and G.A. TETERS, *Strength of solid polymer materials* [in Russian], Riga 1972.
4. M. CZECH, *Description of stress relaxation of the lignostone with the use of the standard model* [in Polish], II Symp. Rheology of Wood and Timber Structures, 69-75, Poznań 1986.
5. B.T. OGARKOV, *Theory of elastic behaviour of wood* [in Russian], Zhur. Tech. Fiz., **27**, 1118–1120, 1957.

BIAŁYSTOK UNIVERSITY OF TECHNOLOGY.

Received December 10, 1994.